Electronic Supplementary Material (ESI) for Environmental Science: Processes & Impacts.
This journal is © The Royal Society of Chemistry 2018

Supporting Information for:

Degradation of polyethylene glycols and polypropylene glycols in microcosms simulating a spill of produced water in shallow groundwater

Jessica D. Rogers[1,2], E. Michael Thurman[1], Imma Ferrer[1], James S. Rosenblum[1], Morgan V. Evans[3], Paula J. Mouser[3,4], and Joseph N. Ryan[1*]
[1] Department of Civil, Environmental and Architectural Engineering
University of Colorado Boulder, Boulder, CO 80309
[2] S.S Papadopulos & Associates, Inc.; Boulder, CO 80303
[3] Department of Civil, Environmental and Geodetic Engineering
The Ohio State University, Columbus, OH 43210
[4] Department of Civil and Environmental Engineering
University of New Hampshire, Durham, NH 03824
* Corresponding author, phone: (303)492-0772; e-mail: joseph.ryan@colorado.edu

Contents:

S1. Methods
S2. MS-MS experiments

Table S1: Summary of well information and fracturing fluid additives reported for well A
Table S2: Summary of well information and fracturing fluid additives reported for well B
Table S3: Sediment properties and composition of synthetic groundwater
Table S4: Summary of water quality data from the COGCC
Table S5: Summary of water quality analysis of shallow groundwater samples
Table S6: Summary of 2012 COGCC spill reports for groundwater–impacting spills
Table S7: Total dissolved solid (TDS) concentrations measured in the day 0 microcosm samples
Table S8: Identification of PEG species and corresponding degradation products
Table S9: Identification of PPG species and corresponding degradation products
Table S10: Microbial community richness and diversity

Figure S1: Rarefaction based on uneven sampling
Figure S2: Rarefaction based on 14,640 sequences/sample
Figure S3: Correlations between 16S rRNA gene copies and *recA* copies
Figure S4: Redox-active species for A-22 microcosms
Figure S5: Redox-active species for A-611 microcosms
Figure S6: Redox-active species for B-14 microcosms
Figure S7: Redox-active species for B-161 microcosms
Figure S8: pH measured in microcosm experiments
Figure S9: Total system ATP in microcosm experiments
Figure S10: Mass spectrum of PEG-9-diCOOH
Figure S11: MS-MS spectrum and fragmentation pathways of PEG-diCOOH
Figure S12: Mass spectrum of PPG-6-COOH
Figure S13: MS-MS spectrum and fragmentation pathway of PPG-COOH
Figure S14: Relative abundance of *Pseudomonas* in the sediment microbial community
Figure S15: Relative response of PPG-4 and PPG-4-COOH in microcosm experiments
Figure S16: Relative response of PEG-9, PEG-9-COOH, and PEG-9-diCOOH

S1. Methods

S1.1 ATP analysis: Suspended and attached adenosine triphosphate (ATP) was quantified for aqueous and sediment samples according to manufacturer instructions[1, 2] using a luminescence assay and luminometer (Quench-Gone-Aqueous and Deposit & Surface Analysis; PhotonMaster, LuminUltra). To extract the suspended ATP, aqueous samples were syringe-filtered and lysed with 1 mL of UltraLyse 7 reagent provided by the manufacturer. The eluent was stored at 4°C and analyzed within 7 d. The eluent was then diluted with 9 mL of UltraLute reagent provided by the manufacturer, and 100 μL of the sample solution was exposed to 100 μL of a luciferase enzyme. A luminometer was used to immediately measure the light output in relative light units (RLUs). For attached ATP, microcosm sediments were homogenized using a stainless steel spatula sterilized with 70% ethanol. Approximately 1 g of sediments was extracted from the serum bottle, and excess water was removed using a vacuum pump and a 47 mm disk filter (0.45 μm, polyethersulfone membrane, Pall Corporation). The mass of the dried sediment was measured using an analytical balance, then the sediments were added to a sterile 15 mL centrifuge tube with 5 mL of the UltraLyse 7 reagent and agitated using a vortex mixer for 30 seconds. The extraction slurry was stored at 4°C and analyzed within 7 d. For analysis, 1 mL of the extraction slurry was diluted with 9 mL of the UltraLute reagent in a fresh 15 mL sterile centrifuge tube; 100 μL of this solution was exposed to 100 μL of a luciferase enzyme, and a luminometer was used to immediately measure the light output. The RLU response was converted to pg ATP mL^{-1} using the RLU response of an ATP standard provided by the manufacturer and corrected for the volume of sample filtered (suspended) or mass of sediment (attached). The detection limit of the method reported by the manufacturer was 10 RLUs,[1] which corresponds to approximately 0.1 pg ATP mL^{-1} (suspended) or 50 pg ATP g^{-1} (attached).

Total system ATP was determined by multiplying the suspended and attached ATP concentration by the total amount of liquids (100 mL) and sediments (20 g, dry weight equivalent) in each microcosm, respectively. The two masses were then summed to determine the total system ATP for each microcosm.

S1.2 Sediments and groundwater composition: Sediments were collected via hand auger between the depths of 0.9 m (depth of the water table) and 2.5 m from a surficial aquifer adjacent to the South Platte River in the Denver-Julesburg Basin. There were 18 oil and gas production wells within 1 km of the sediment collection site; thus, the sediments are representative of a surficial aquifer susceptible to contamination from a release of produced water. Quaternary deposits along stream channels in the South Platte River Basin form unconfined alluvial aquifers where saturated: These formations are characterized as unconsolidated, coarse-grain sand and gravel with interbedded clays in some areas.[3] Sediments were collected via hand auger from two adjacent boreholes, homogenized, sieved through a 2 mm mesh, and stored saturated with native groundwater at 4°C. Sediment properties are summarized in Table S3. Organic carbon (OC) content was determined by loss on ignition conducted with 25 g sub-samples. Major elemental composition was determined by acid digestion followed by inductively-coupled plasma optical emission spectrometry (model 3410+, Applied Research Laboratories). Attached ATP was measured as described in S1.1.

A synthetic groundwater representative of Denver-Julesburg Basin alluvial aquifers with respect to major ions and pH was used in all microcosms (Table S3). Following a rigorous quality control screening described by Sherwood et al.,[4] the synthetic groundwater composition was determined using publically-available data from the Colorado Oil and Gas Conservation

Commission (COGCC). Water quality data were examined from 124 unique water wells (n = 220 samples) completed in "Quaternary alluvium" formations within the Denver-Julesburg Basin (Table S4). Additionally, groundwater samples were collected from the two hand-auger boreholes used to collect the sediments and analyzed for water quality (Table S5). The major ion composition of the shallow groundwater in the boreholes was consistent with the COGCC data set, with the exception of nitrate and sulfate, which were 1-2 standard deviations higher than the median concentrations of the COGCC data. Local groundwater samples were also analyzed for dissolved organic carbon (DOC), suspended adenosine triphosphate (ATP), and BTEX (benzene, toluene, ethylbenzene, and xylenes). DOC was quantified by high-temperature combustion (TOC-L_{CPN}, Shimadzu Corporation) and BTEX was analyzed using purge and trap gas chromatography-mass spectrometry by a commercial laboratory following EPA method SW-846. While the BTEX compounds were all non-detect, DOC was somewhat high at 5.8 mg L^{-1}, and ATP results indicated significant biological activity in the native groundwater (Table S5). The high DOC and nitrate levels may be due to interaction with the surface water in the nearby South Platte River.[5]

Major ion concentrations and pH of the synthetic groundwater were determined using the chemical equilibrium software Visual MINTEQ,[6] applying targets of median values from the COGCC dataset and assuming equilibrium with the atmosphere. The target concentrations of nitrate and sulfate were increased to be consistent with concentrations measured in the local groundwater samples to ensure that biodegradation by the native microbial consortium on the sediments was not limited by electron-acceptor availability. The synthetic groundwater was mixed using high-purity water (≥18 MΩ cm resistivity) and was autoclaved prior to experiments. All salts were of reagent-grade purity (Fisher Scientific).

Samples for major anions and cations analysis were syringe-filtered (0.2 μm, polyethersulfone membrane, Pall Corporation). Cation samples were preserved with 1% nitric acid and analyzed using inductively coupled plasma-optical emission spectroscopy (model 3410+, Applied Research Laboratories). A blank and three standards made with dilutions of certified standards were used for calibrations, with detection limits of 5 and 10 ppb for total manganese and total iron, respectively. Anions were analyzed by ion chromatography (model 4500I, Dionex). Separation was achieved with an AG14 guard column and AS14 anion-exchange column (Dionex), using a Na_2CO_3-$NaHCO_3$ eluent at a flow rate of 1.2 mL min^{-1}. Four NIST traceable standards were used for calibration, with detection limits of 10, 100, and 50 ppb for nitrite, nitrate, and sulfate, respectively.

S1.3 Denver-Julesburg Basin surface spill analysis: Dilution factors for each produced water were determined to normalize the initial benzene concentration in the microcosms to 1 mg L^{-1}, which was representative of benzene concentrations measured in shallow groundwater immediately following surface spills of produced water in the Denver-Julesburg Basin. Concentrations of ethoxylated surfactants in groundwater following a surface spill are not readily available, so benzene concentrations, which are commonly measured, were used estimate the extent that the released produced water would be diluted with native groundwater during a surface spill. Spill data from the COGCC was used to determine typical benzene concentrations following surface spills of Denver-Julesburg Basin produced water. Denver-Julesburg Basin spill records from the year 2012 were collected and analyzed as described by Armstrong et al.[7] Of the spills determined to have impacted groundwater (n = 84), those where produced water was reported as the only released material were selected (n = 10, 12% of total groundwater-

impacting spills in 2012). The supporting documents (e.g., consultant reports, laboratory results) for these spills were reviewed to identify the highest initial benzene concentration measured in groundwater after the spill was first reported. Benzene concentrations ranged from non-detect to 4.1 mg L^{-1}, with a median of 0.3 mg L^{-1} and an average of 0.9 mg L^{-1} (Table S6).

The dilution factors of the four produced water treatments ranged from 7 to 12× depending on the concentration of benzene in the sample collected from each well: A-22 was diluted by a factor of 7.0, A-611 by a factor of 12, B-14 by a factor of 7.4 and B-161 by a factor of 10.

S2. MS-MS experiments

S2.1 PEG-diCOOH: The MS-MS spectrum and fragmentation pathways for the peak at 9.2 min corresponding to the putative identification of PEG-6-diCOOH are show in Figure S11. Two pathways were observed. In pathway one, there is an initial loss of one terminal carboxyl group as formic acid (-46.0057 mass units) to yield the MH+ ion at *m/z* 265.1285, which subsequently losses formaldehyde (-30.0109 mass units) to yield the MH+ ion at *m/z* 235.1176. The molecule is then "unzipped" with a series of losses of 44 mass units to give major ions at *m/z* 191.0917, 147.14065, and 103.0392. The 44 mass unit loss corresponds to the ethylene oxide unit (CH_2CH_2O). The second pathway begins with an initial loss of a terminal carboxyl group as glyoxal (-58.0059 mass units), followed by loss of the second terminal carboxyl group as formic acid (-46 mass units). The molecule is then "unzipped" by a series of 44 mass unit losses to give major ions at *m/z* 163.096, 119.0704, and 87.0445. A PEG-6-diCOOH standard was not available; thus, the identification remains unconfirmed.

S2.2 PPG-COOH: The MS-MS spectrum and fragmentation pathway for the peak at 17.6 min corresponding to the putative identification of PPG-7-COOH are shown in Figure S13. There is an initial loss of a terminal dipropylene glycol (-134.0943 mass units) from the non-oxidized end of the molecule to yield the MH+ ion at *m/z* 305.1950. The molecule then "unzips" with a series of 58 mass unit losses to give ions at *m/z* 247.1536, 189.1117, and 131.0702. The 58 mass unit loss corresponds to the propylene oxide unit ($CH_2CH(CH_3)O$). The final two steps are a loss of 28 mass units (CO), followed by a loss of an ethylene oxide (-44 mass units, CH_2CH_2O) to yield the propylene oxide monomer (*m/z* 59.4093). A PPG-7-COOH standard was not available; thus, the identification remains unconfirmed.

Table S1. Summary of well information from the COGCC and fracturing fluid additives identified on the FracFocus report for well A. The FracFocus report provides the purpose of additives used in the fracturing fluid as well as non-proprietary specific ingredients used in each.

summary of well information				
vertical depth (m)	2,150			
base water volume (L)	1.10×10^7			
num. stages	28			
target formation	Niobrara			
fracturing fluid additives				
purpose	**ingredient**	**CAS**	**max. ingredient conc. in additive (% by mass)**	**max ingredient conc. in HF fluid (% by mass)**
carrier	water	7732-18-5	100.0	84.9923
sand	crystalline silica (quartz)	14808-60-7	99.9	14.1534
guar slurry (CMHPG)	petroleum distillate	64742-47-8	55.0	0.1896
	guar gum	9000-30-0	50.0	0.1723
	clay	proprietary	5.0	0.0172
peroxide breaker	ethylene glycol	107-21-1	40.0	0.0762
	tert-butyl hydroperoxide	75-91-2	10.0	0.0190
clay stabilizer	trade secret	proprietary	100.0	0.0524
non-emulsifier	proprietary surfactants	68439-46-3	20.0	0.0170
	methanol	67-56-1	15.0	0.0123
	D-Limonene	5989-27-5	10.0	0.0085
	light aromatic naphtha	64742-95-6	5.0	0.0043
breaker accelerator	water	7732-18-5	85	0.0341
	EDTA, diammonium copper salt	14025-15-1	15.0	0.0060
crosslinker	zirconium solution	proprietary	60.0	0.0184
pH buffer	acetic acid	64-19-7	80.0	0.0157
biocide	polyethylene glycol	25322-68-3	50.0	0.0058
	water	7732-18-5	30.0	0.0035
	2,2-dibromo-3-nitrilpropionamide	10222-01-2	20.0	0.0023
friction reducer	petroleum distillates, hydrotreated light	64742-47-8	30.0	0.0103
solvent	hydrochloric acid	7647-01-0	30.0	0.0100

Table S2. Summary of well information from the COGCC and fracturing fluid additives identified on the FracFocus report for well B.

summary of well information				
vertical depth (m)	2,100			
base water volume (L)	1.60×10^7			
num. stages	33			
target formation	Niobrara			
fracturing fluid additives				
purpose	**ingredient**	**CAS**	**max. ingredient conc. in additive (% by mass)**	**max ingredient conc. in HF fluid (% by mass)**
carrier	water	7732-18-5	100.0	80.9306
sand	crystalline silica (quartz)	14808-60-7	99.9	18.4876
guar slurry	petroleum distillates blend	proprietary	65.0	0.1324
crosslinker	paraffinic naphthenic solvent blend	64742-47-8	65.0	0.0552
	inorganic borates	proprietary	40.0	0.0339
emulsifier	isopropyl alcohol	67-63-0	30.0	0.0495
	citrus terpenes	68647-72-3	5.0	0.0083
friction reducer	copolymer of acrylamide and sodium acrylate	25987-30-8	31.0	0.0085
	isoparaffinic solvent	64742-47-8	31.0	0.0085
	water	7732-18-5	28.5	0.0078
	surfactant blend	proprietary	5.0	0.0014
	ethylene glycol	107-21-1	3.0	0.0008
	sodium acetate	127-09-3	1.5	0.004
pH buffer	sodium hydroxide solution	1310-73-2	30.0	0.0122
	potassium hydroxide solution	1310-58-3	30.0	0.0122
biocide	water	7732-18-5	83.0	0.0135
	glutaraldehyde	111-3-8	14.0	0.0023
	quaternary ammonium compounds	68424-85-1	2.5	0.0004
	ethanol	64-17-5	0.3	0.0001
gel breaker	tert-butyl hydroperoxide	75-91-2	10.0	0.0025
cleanup solution	naphtha (petroleum) hydrotreated heavy	64742-96-7	100.0	0.0007

Table S3. Surficial aquifer sediment properties and composition of synthetic groundwater used in all microcosms.

sediment		**synthetic groundwater**	
organic carbon (OC) content	0.37 ± 0.01 % w/w	pH	7.5
ATP	26,700 ±2,590 pg g^{-1}	Cl^-	150 mg L^{-1}
		HCO_3^-	12 mg L^{-1}
bulk composition	wt. % oxides [a]	SO_4^{2-}	450 mg L^{-1}
SiO_2	70.1	NO_3^-	17 mg L^{-1}
Al_2O_3	11.3	PO_4^{3-}	2.0 mg L^{-1}
K_2O	6.9	Na^+	100 mg L^{-1}
Fe_2O_3	6.2	K^+	5.0 mg L^{-1}
NaO_2	2.8	Mg^{2+}	65 mg L^{-1}
CaO	1.3	Ca^{2+}	86 mg L^{-1}
TiO_2	0.8	NaN_3 [b]	5.0 g L^{-1}
MgO	0.5		
MnO	0.1		
P_2O_5	0.1		

[a] Elements assumed to be present as oxides.
[b] Added to abiotic controls.

Table S4. Summary of water quality data from the COGCC used to determine the synthetic groundwater composition used in all microcosms. Data is from 124 unique water wells (*n* = 220 samples) screened in "quaternary alluvium" formations within the Denver-Julesburg Basin.

parameter	median (mg L^{-1})	range		n samples [a]
		min (mg L^{-1})	max (mg L^{-1})	
pH	7.5	6.6	9.4	104
Cl^-	120	3.9	570	119
HCO_3 alkalinity	270	44	590	121
Br^-	0.48	0.0	1.7	93
SO_4^{2-}	360	1.0	2,200	118
NO_3^-	5.4	0.0	43	68
PO_4^{3-}	2.0 [b]	n/a	n/a	0
Na^+	140	0.0	510	117
K^+	5.2	0.0	52	112
Total Fe	0.0	0.0	5.0	108
Total Mn	0.0	0.0	1.9	105
Mg^{2+}	44	0.0	180	112
Ca^{2+}	110	1.1	1,000	112

[a] Number of samples for which the parameter was reported.

[b] Phosphate data not reported in COGCC samples. Target value of 2 mg L^{-1} determined from a report of water quality in Denver-Julesburg Basin alluvial aquifers.[5]

Table S5. Summary of water quality analysis of shallow groundwater samples from two hand-auger boreholes used to collect the alluvial aquifer sediments.

parameter	borehole 1	borehole 2	average
pH	7.2	7.2	7.2
DO (mg L^{-1})	5.8	5.8	5.8
ATP (pg mL^{-1})	1,900	1,820	1,860
BTEX compounds [a]	nd	nd	nd
Cl^- (mg L^{-1})	95.1	94.3	94.7
Br^- (mg L^{-1})	0.00	0.17	0.09
SO_4^{2-} (mg L^{-1})	494	474	484
NO_3^- (mg L^{-1})	36.3	20.5	28.4
PO_4^{3-} (mg L^{-1})	0.43	1.78	1.1
Na^+ (mg L^{-1})	141	151	146
K^+ (mg L^{-1})	2.05	1.85	1.95
Total Fe (mg L^{-1})	0.12	0.31	0.22
Total Mn (mg L^{-1})	0.004	0.014	0.009
Mg^{2+} (mg L^{-1})	87.2	85.3	86.3
Ca^{2+} (mg L^{-1})	181	176	178

[a] Groundwater collected from sediment boreholes were analyzed for the presence of BTEX compounds (benzene, toluene, ethylbenzene and xylenes). Both samples were found to be non-detect (nd) for all BTEX compounds.

Table S6. Summary of 2012 COGCC spill reports for groundwater (gw) –impacting spills which reported produced water as the only released material.

COGCC report num. [a]	incident date	impacted media	depth to gw (m)	sample location	max. initial benzene conc. (mg L^{-1}) [b]
2314598	23-Jan-12	gw, soils	4.0	monitoring well	1.7
2223195	5-Mar-12	gw, soils	1.8	monitoring well	0.10
2229553	2-Apr-12	gw, soils	3.1	monitoring well	4.1
2230160	11-May-12	gw, soils	1.5	monitoring well	nd [c]
2230986	19-Jun-12	gw, soils	1.8	monitoring well	0.85
2229570	25-Jun-12	gw, soils	3.1	monitoring well	0.33
2229552	9-Jul-12	gw, soils	1.5	soil bore	0.63
2141611	22-Aug-12	gw, soils	2.1	excavation pit	0.18
2145176	15-Nov-12	gw, soils	2.1	excavation pit	0.14
2146028	13-Dec-12	gw, soils	1.2	excavation pit	0.02

[a] Number assigned by the COGCC to identify the remediation report file.
[b] Highest initial benzene concentration measured in groundwater after the spill was first reported.
[c] Non-detect (nd)

Table S7. Total dissolved solid (TDS) concentrations measured in the day 0 sample for each of the produced water microcosm experiments.

microcosm	TDS (mg L^{-1})
A-22	3,260
A-611	1,970
B-14	1,920
B-161	2,360

Table S8. Identification of PEG species and corresponding degradation products.

compound	RT [a] (min)	putative formula	calculated exact mass (m/z) $[Na^+]$ [b]	measured exact mass (m/z)	error (ppm)
PEG					
PEG-3	3.8	$C_6H_{14}O_4$	173.0784	173.0786	1.16
PEG-4	4.2	$C_8H_{18}O_5$	217.1046	217.1048	0.92
PEG-5	5.8	$C_{10}H_{22}O_6$	261.1309	261.1309	0.00
PEG-6	7.8	$C_{12}H_{26}O_7$	305.1571	305.1573	0.66
PEG-7	9.7	$C_{14}H_{30}O_8$	349.1833	349.1837	1.15
PEG-8	10.5	$C_{16}H_{34}O_9$	393.2095	393.2097	0.51
PEG-9	10.9	$C_{18}H_{38}O_{10}$	437.2357	437.2362	1.14
PEG-10	11.3	$C_{20}H_{42}O_{11}$	481.2619	481.2626	1.45
PEG-11	11.6	$C_{22}H_{46}O_{12}$	525.2881	525.2886	0.95
PEG-12	11.9	$C_{24}H_{50}O_{13}$	569.3144	569.3148	0.70
PEG-13	12.1	$C_{26}H_{54}O_{14}$	613.3406	613.3410	0.65
PEG-14	12.3	$C_{28}H_{58}O_{15}$	657.3668	657.3669	0.15
PEG-COOH					
PEG-4-COOH	4.7	$C_8H_{16}O_6$	231.0839	231.0841	0.87
PEG-5-COOH	6.2	$C_{10}H_{20}O_7$	275.1101	275.1104	1.09
PEG-6-COOH	8.5	$C_{12}H_{24}O_8$	319.1363	319.1363	0.00
PEG-7-COOH	10.0	$C_{14}H_{28}O_9$	363.1626	363.1627	0.28
PEG-8-COOH	10.7	$C_{16}H_{32}O_{10}$	407.1888	407.1889	0.25
PEG-9-COOH	11.1	$C_{18}H_{36}O_{11}$	451.2150	451.2150	0.00
PEG-10-COOH	11.5	$C_{20}H_{40}O_{12}$	495.2412	495.2413	0.20
PEG-11-COOH	11.8	$C_{22}H_{44}O_{13}$	539.2674	539.2673	-0.19
PEG-12-COOH	12.1	$C_{24}H_{48}O_{14}$	583.2936	583.2936	0.00
PEG-13-COOH	12.3	$C_{26}H_{52}O_{15}$	627.3198	627.3193	-0.80
PEG-14-COOH	12.5	$C_{28}H_{56}O_{16}$	671.3461	671.3458	-0.45
PEG-diCOOH					
PEG-4-diCOOH	4.9	$C_8H_{14}O_7$	245.0632	245.0634	0.82
PEG-5-diCOOH	6.7	$C_{10}H_{18}O_8$	289.0894	289.0895	0.35
PEG-6-diCOOH	9.2	$C_{12}H_{22}O_9$	333.1156	333.1158	0.60
PEG-7-diCOOH	10.3	$C_{14}H_{26}O_{10}$	377.1418	377.1419	0.27
PEG-8-diCOOH	10.9	$C_{16}H_{30}O_{11}$	421.1680	421.1686	1.42
PEG-9-diCOOH	11.4	$C_{18}H_{34}O_{12}$	465.1942	465.1947	1.07
PEG-10-diCOOH	11.7	$C_{20}H_{38}O_{13}$	509.2205	509.2209	0.79
PEG-11-diCOOH	12.0	$C_{22}H_{42}O_{14}$	553.2467	553.2469	0.36
PEG-12-diCOOH	12.3	$C_{24}H_{46}O_{15}$	597.2729	597.2731	0.33
PEG-13-diCOOH	12.5	$C_{26}H_{50}O_{16}$	641.2991	641.2992	0.16
PEG-14-diCOOH	12.7	$C_{28}H_{54}O_{17}$	685.3253	685.3254	0.15

[a] Retention time

[b] Calculated exact mass reported for sodium (Na^+) adduct

Table S9. Identification of PPG species and corresponding degradation products.

compound	RT [a] (min)	putative formula	calculated exact mass (m/z) $[Na^+]$ [b]	measured exact mass (m/z)	error (ppm)
PPG					
PPG-2	5.2	$C_6H_{14}O_3$	157.0835	157.0837	-1.27
PPG-3	10.8	$C_9H_{20}O_4$	215.1254	215.1258	1.86
PPG-4	13.1	$C_{12}H_{26}O_5$	273.1672	273.1675	1.10
PPG-5	14.6	$C_{15}H_{32}O_6$	331.2092	331.2093	0.30
PPG-6	16.0	$C_{18}H_{38}O_7$	389.2510	389.2513	0.77
PPG-7	17.3	$C_{21}H_{44}O_8$	447.2928	447.2934	1.34
PPG-8	18.5	$C_{24}H_{50}O_9$	505.3347	505.3355	1.58
PPG-9	19.7	$C_{27}H_{56}O_{10}$	563.3766	563.3774	1.42
PPG-10	20.9	$C_{30}H_{62}O_{11}$	621.4184	621.4195	1.77
PPG-COOH					
PPG-3-COOH	11.0	$C_9H_{18}O_5$	229.1046	229.1049	1.31
PPG-4-COOH	13.3	$C_{12}H_{24}O_6$	287.1465	287.1469	1.39
PPG-5-COOH	15.0	$C_{15}H_{30}O_7$	345.1884	345.1886	0.58
PPG-6-COOH	16.3	$C_{18}H_{36}O_8$	403.2302	403.2302	0.00
PPG-7-COOH	17.6	$C_{21}H_{42}O_9$	461.2721	461.2719	-0.43
PPG-8-COOH	18.8	$C_{24}H_{48}O_{10}$	519.3140	519.3139	-0.19
PPG-9-COOH	19.8	$C_{27}H_{54}O_{11}$	577.3558	577.3560	0.35
PPG-10-COOH	21.0	$C_{30}H_{60}O_{12}$	635.3977	635.3975	-0.31

[a] Retention time
[b] Calculated exact mass reported for sodium (Na^+) adduct

Table S10. Microbial community richness and diversity. For each sample average of replicates are reported with ± the standard deviation.

produced water	time (d)	sequence counts	H [a]	OTUs
aquifer sediment [b]		36,203 ± 1,348	10.0 ± 0.06	3,546 ± 1
A-22	0	67,744	10.06	4,269
	1	37,933 ± 1,900	5.50 ± 0.13	1,952 ± 41
	3	50,912 ± 17,212	6.51 ± 0.72	2,132 ± 499
	21	43,242 ± 19,408	6.13 ± 0.22	1,697 ± 435
	49	42,108 ± 11,068	6.61 ± 0.10	1,835 ± 285
	86	54,827 ± 16,049	6.68 ± 0.16	2,037 ± 311
A-650	0	65,068	10.08	3,978
	1	39,648 ± 14,783	8.53 ± 0.40	2,905 ± 481
	3	39,213 ± 9,788	5.90 ± 0.51	2,073 ± 435
	21	34,715 ± 4,925	7.19 ± 0.07	2,262 ± 178
	49	29,603 ± 8,240	7.41 ± 0.17	2,036 ± 236
	86	23,984 ± 2,971	6.57 ± 0.51	1,683 ± 243
B-14	0	29,024	9.67	2,953
	1	26,154 ± 10,357	6.26 ± 0.65	1,558 ± 143
	4	29,343 ± 5,053	5.66 ± 0.07	1,316 ± 25
	20	36,656 ± 4,312	6.00 ± 0.25	1,543 ± 62
	47	25,840 ± 5,719	5.80 ± 0.17	1,320 ± 126
	90	64,941 ± 11,936	5.99 ± 0.05	2,191 ± 175

[a] Shannon's diversity index
[b] Aquifer sediments prior to exposure to produced water

Figure S1. Rarefaction based on uneven sampling**.**

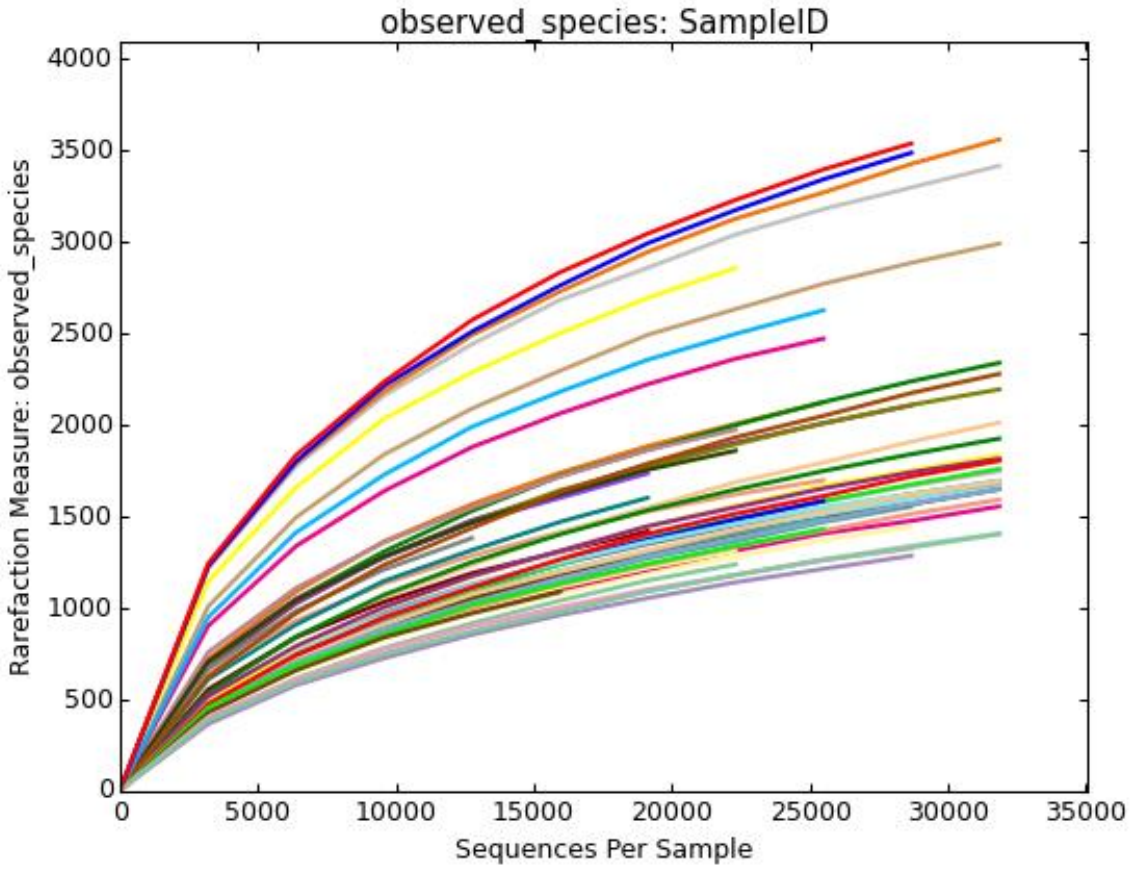

Figure S2. Rarefaction based on 14,640 sequences/sample.

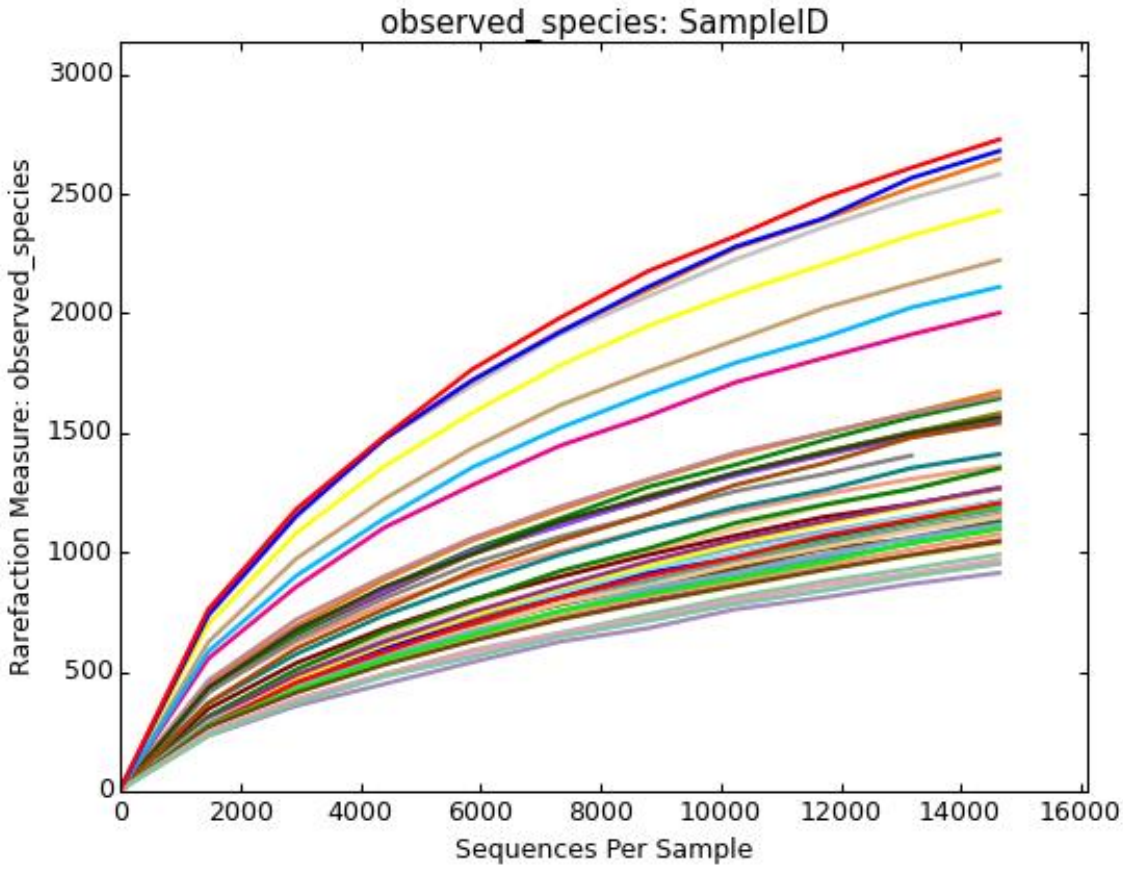

Figure S3. Correlations between 16S rRNA gene copies and *recA* copies per sample in the A-22 (orange), A-611 (blue), and B-14 (grey) microcosm samples, as predicted in metagenomes using PiCRUST analysis.

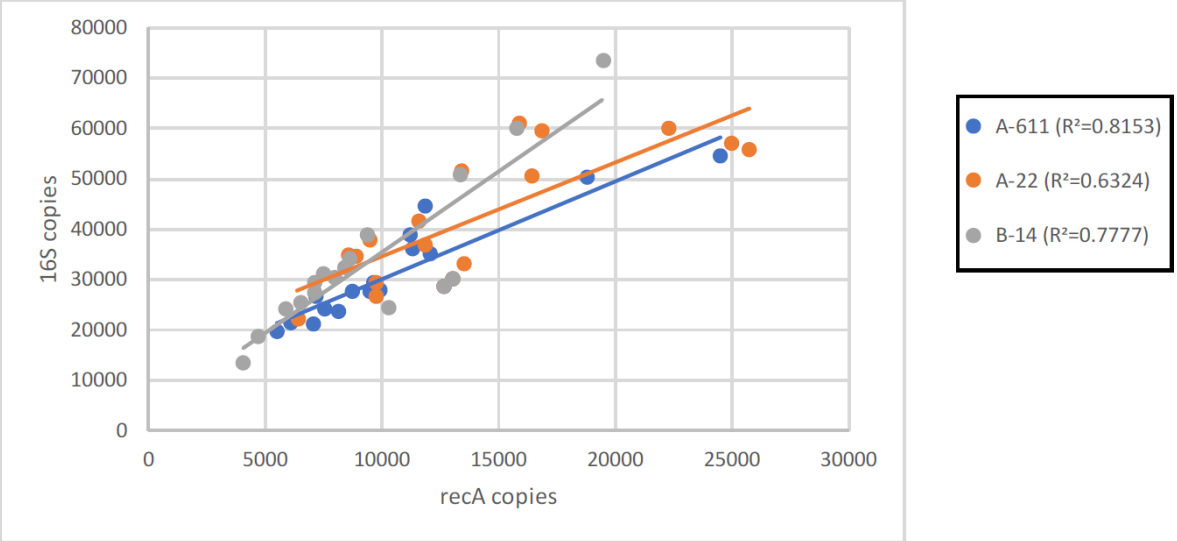

Figure S4. Redox active species for the (a) biologically active and (b) abiotic A-22 microcosms. Dissolved oxygen (DO; blue), nitrate (NO_3^-, green), nitrite (NO_2^-, grey), total manganese (Mn; purple), total iron (Fe; red), and sulfate (SO_4^{2-}; yellow) are plotted *vs.* time. The black dashed line indicates the oxic/anoxic transition (3 d for A-22), defined as the time when DO was depleted. DO was considered depleted at 1.5 mg L^{-1} due to the sampling procedure, in which it was not possible to eliminate all opportunities for re-oxygenation of the sample. NO_3^- is not shown for the abiotic control column due to analytical interferences with sodium azide.

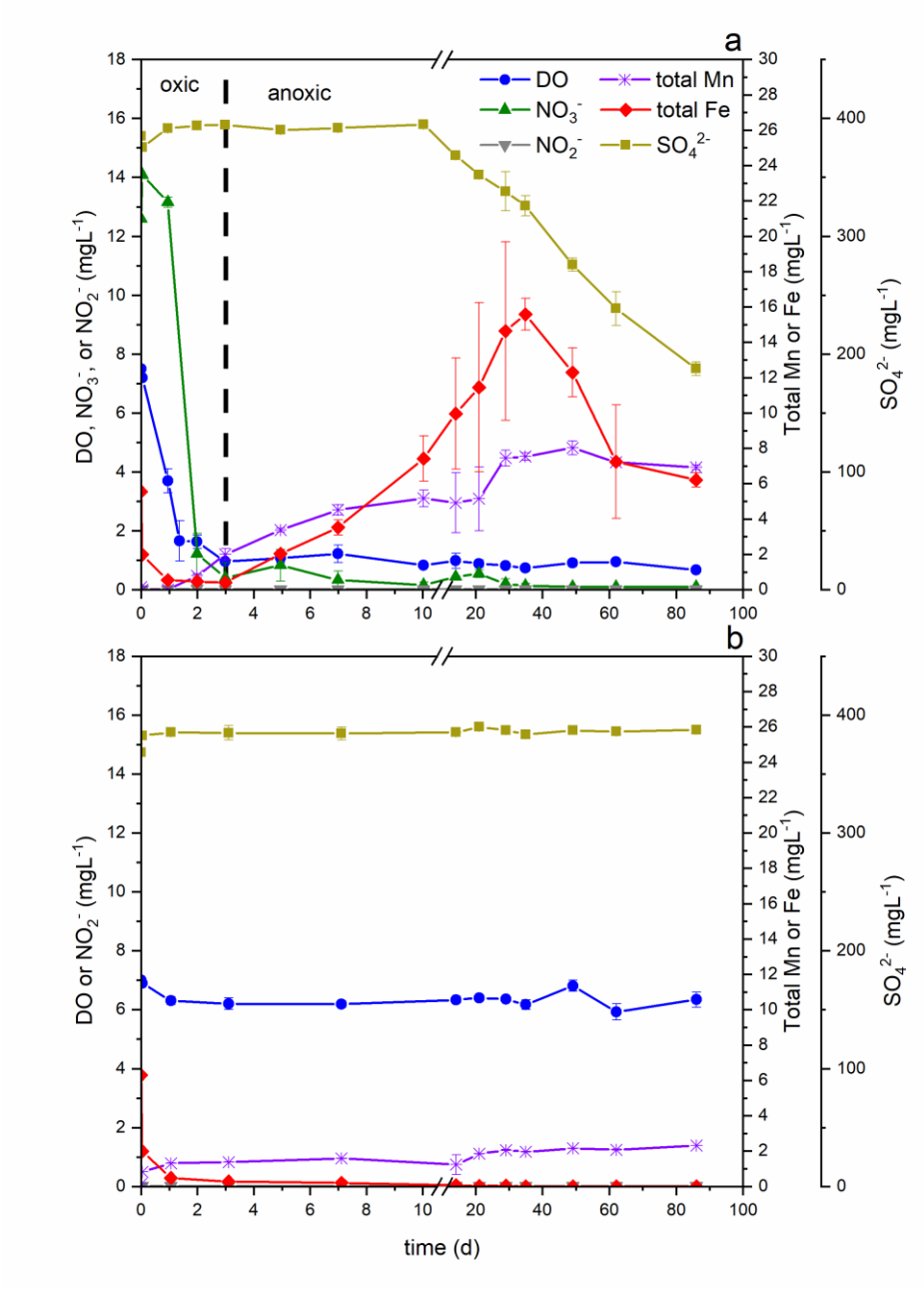

Figure S5. Redox active species for the (a) biologically active and (b) abiotic A-611 microcosms. Dissolved oxygen (DO; blue), nitrate (NO_3^-, green), nitrite (NO_2^-; grey), total manganese (Mn; purple), total iron (Fe; red), and sulfate (SO_4^{2-}; yellow) are plotted *vs.* time. The black dashed line indicates the oxic/anoxic transition (21 d for A-611).

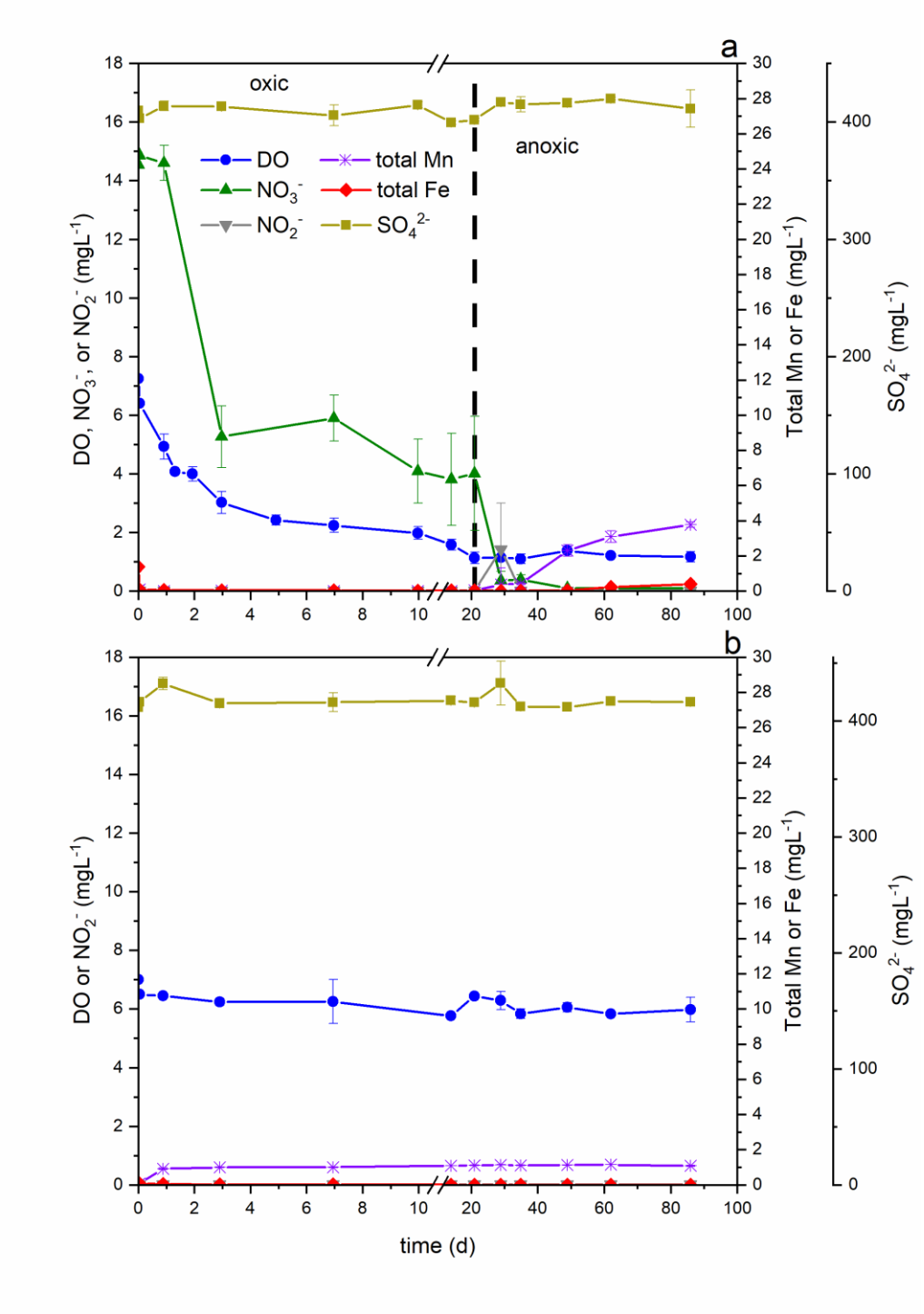

Figure S6. Redox active species for the (a) biologically active and (b) abiotic B-14 microcosms. Dissolved oxygen (DO; blue), nitrate (NO_3^-, green), nitrite (NO_2^-; grey), total manganese (Mn; purple), total iron (Fe; red), and sulfate (SO_4^{2-}; yellow) are plotted *vs.* time. The black dashed line indicates the oxic/anoxic transition (4 d for B-14).

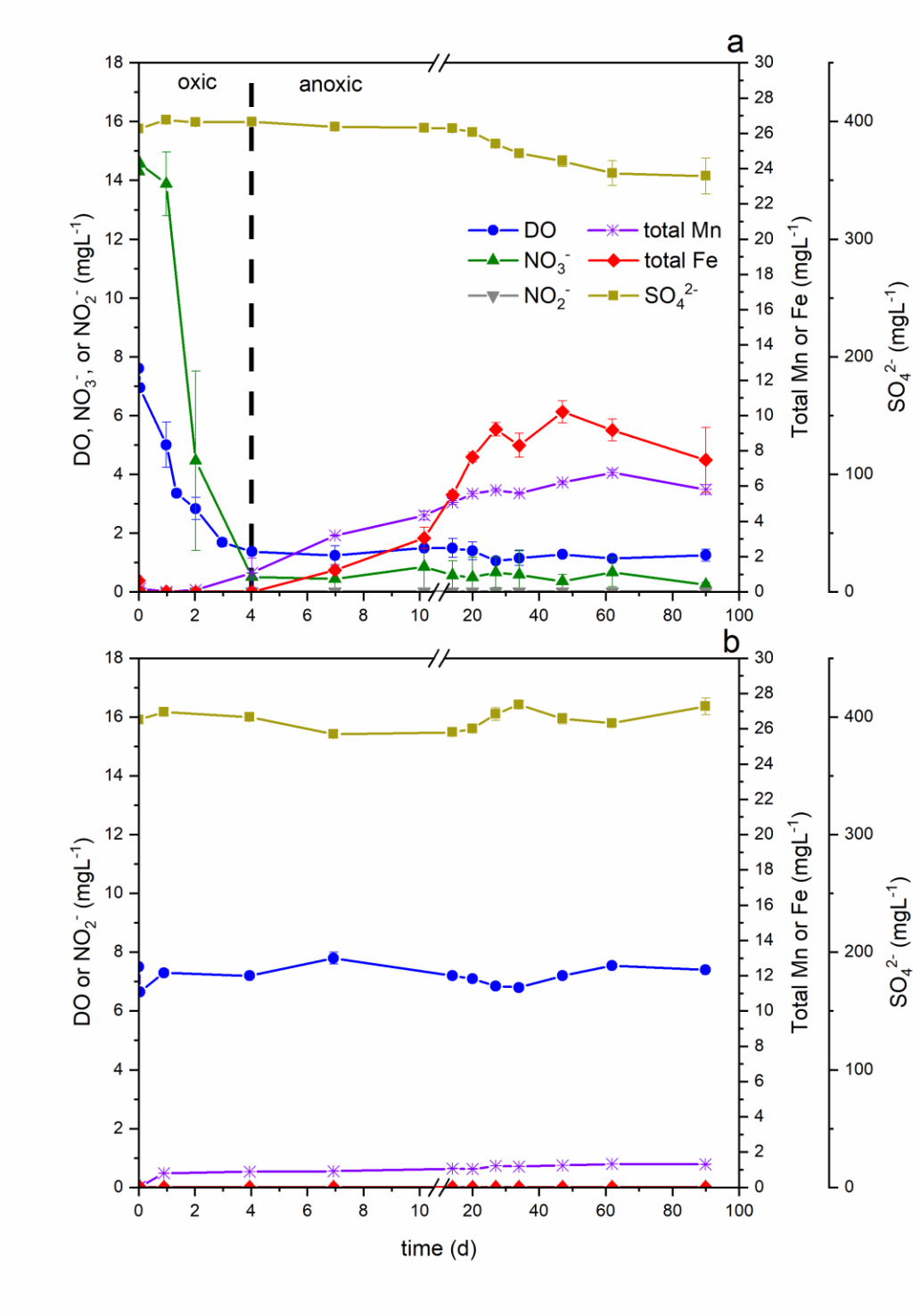

Figure S7. Redox active species for the (a) biologically active and (b) abiotic B-161 microcosms. Dissolved oxygen (DO; blue), nitrate (NO_3^-, green), nitrite (NO_2^-; grey), total manganese (Mn; purple), total iron (Fe; red), and sulfate (SO_4^{2-}; yellow) are plotted *vs.* time. The black dashed line indicates the oxic/anoxic transition (28 d for B-161).

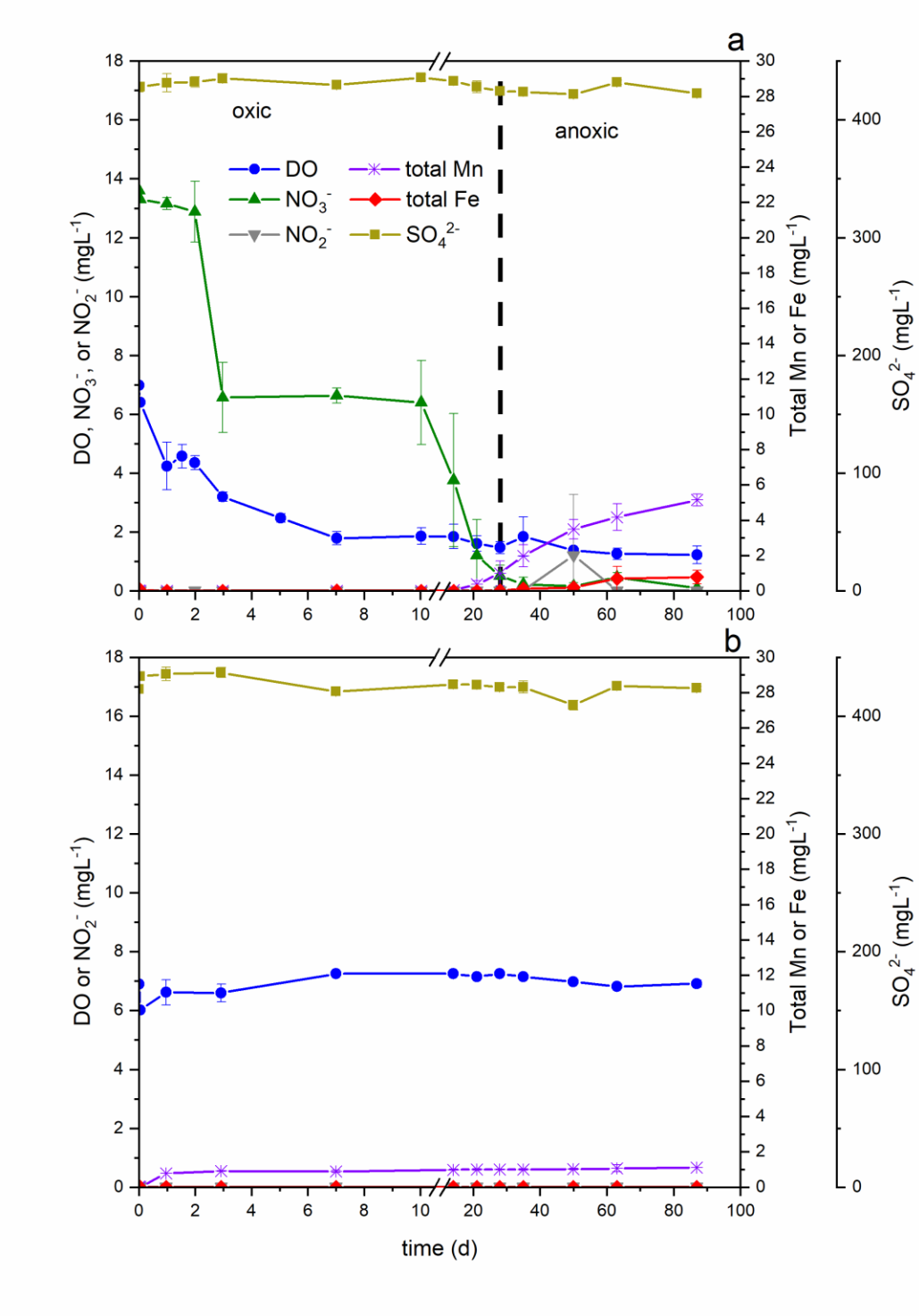

Figure S8. pH *vs.* time in the A-22 (diamond symbols), A-611 (triangle symbols), B-14 (square symbols), and B-161 (circle symbols) microcosm experiments.

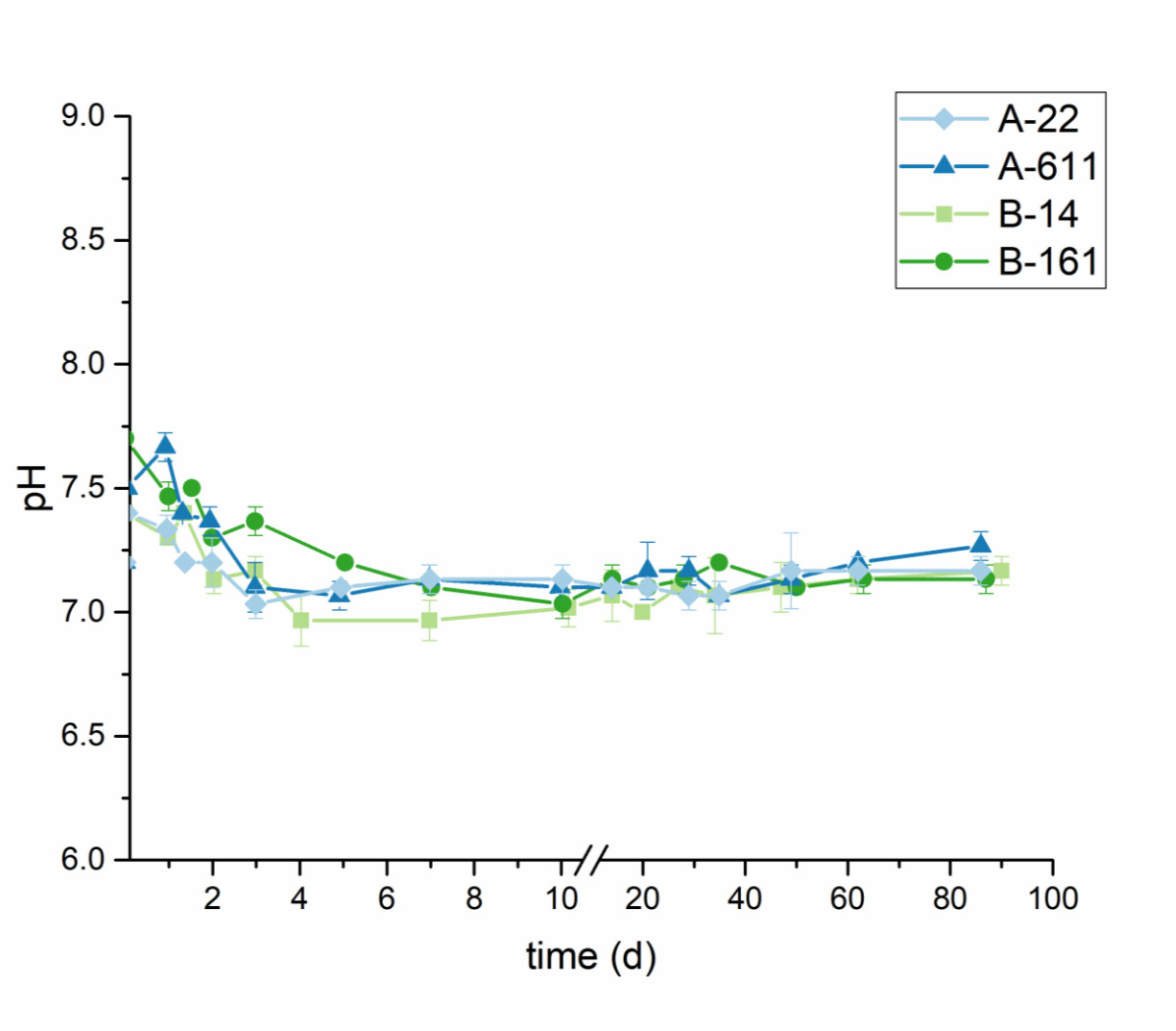

Figure S9. Total system (suspended and attached) ATP in (a) A-22, (b) A-611, (c) B-14, and (d) B-161 microcosms. Open symbols represent abiotic controls and filled symbols represent the biologically active microcosms. The detection limit for the total system ATP was 1000 pg. An axis break at d 10 is used to show detail corresponding to the period of rapid degradation.

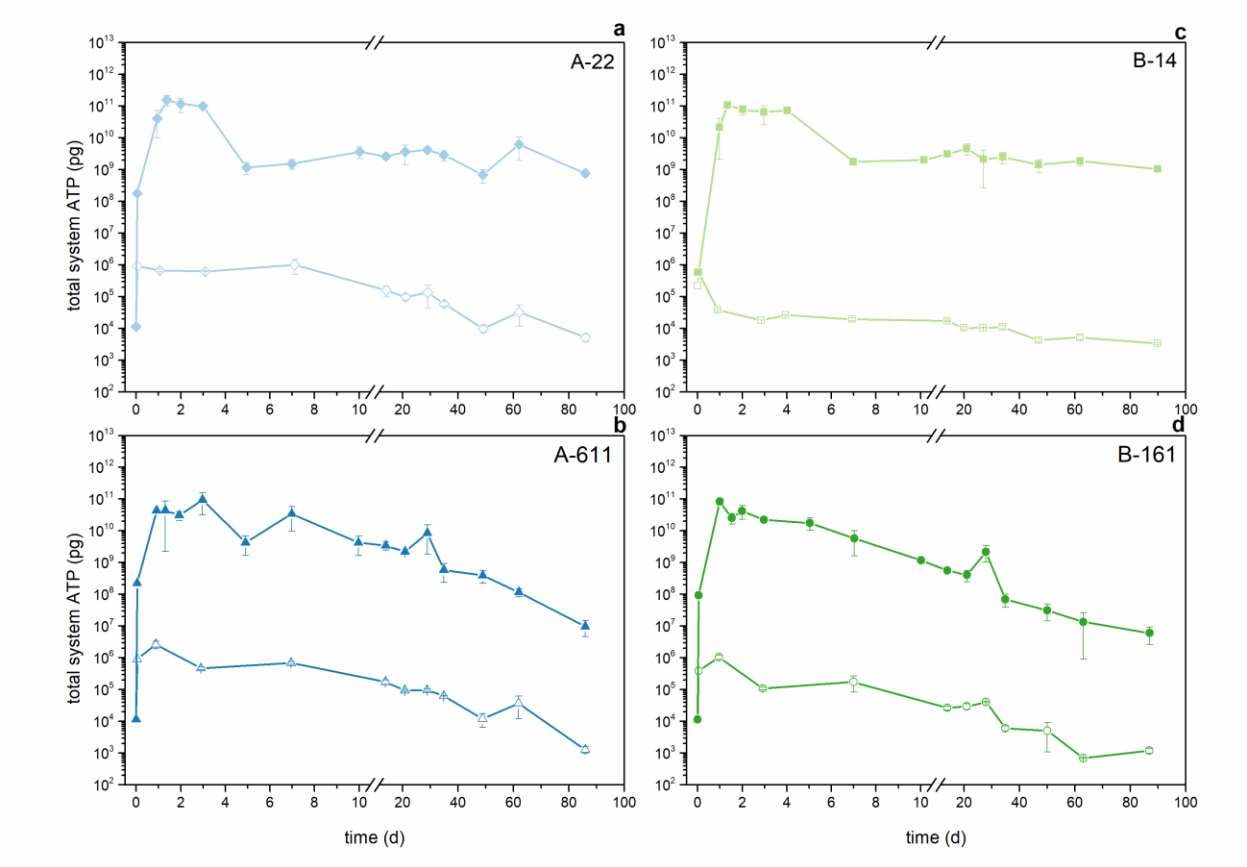

Figure S10. Mass spectrum of PEG-9-diCOOH. The ammonium (*m/z* 460.2396), sodium (*m/z* 465.1947), and proton (*m/z* 443.2126) adducts are all present. Double (*m/z* 487.1764) and triple (*m/z* 509.1582) sodium adducts occur when one or both of the carboxyl groups, respectively, are in the form of a sodium salt.

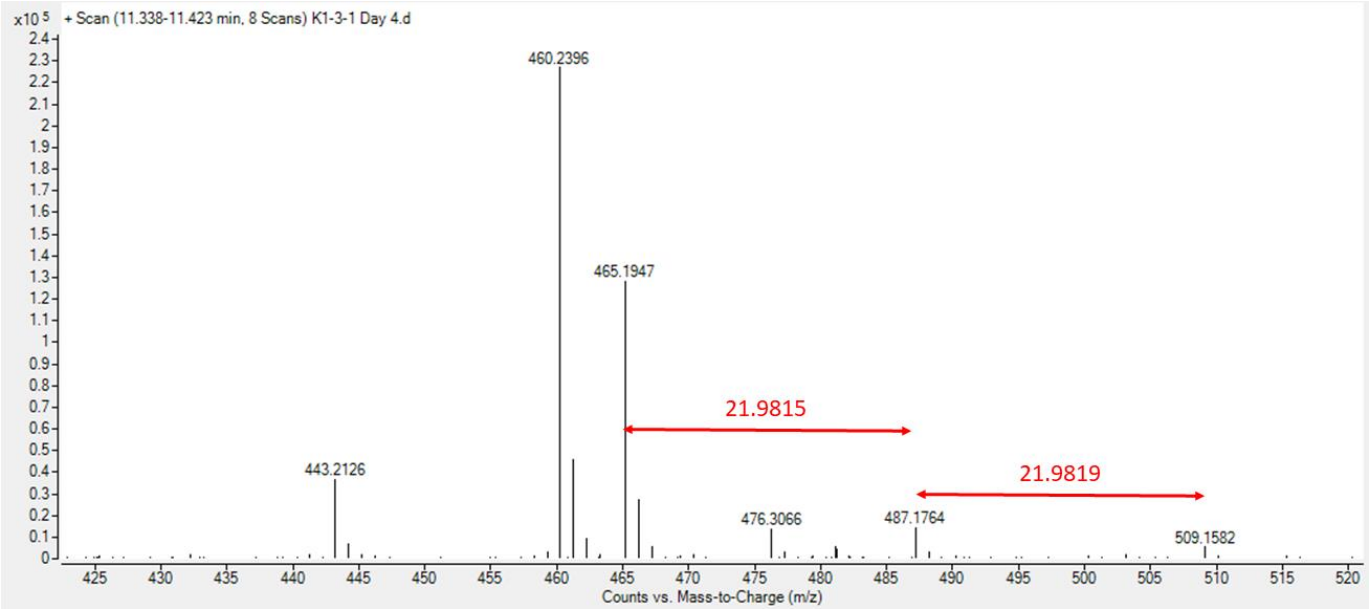

Figure S11. MS-MS of PEG-6-diCOOH for the proton adduct (*m/z* 311). Fragmentation pathway 1 is shown in blue and pathway 2 is shown in red.

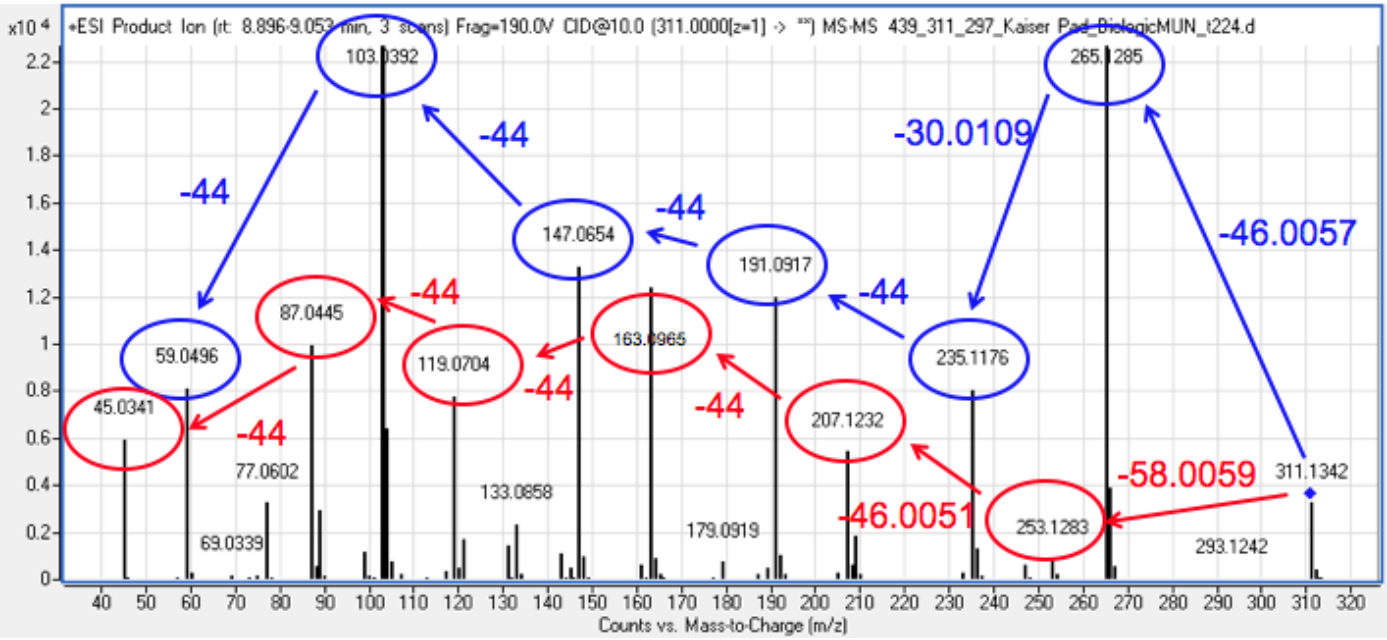

Figure S12. Mass spectrum of PPG-6-COOH. The sodium (*m/z* 403.2302), proton (*m/z* 381.2483), and ammonium (*m/z* 398.2749) adducts are all present. A double (*m/z* 425.2129) sodium adduct indicates the presence of the carboxyl group in the form of a sodium salt, though the response was very small (zoomed inset). Because the PPG-6-COOH peak overlaps with PPG-6, PPG-6 adducts are also visible (e.g., m/z 389.2512 and 384.2956 are the PPG-6 sodium and ammonium adducts, respectively).

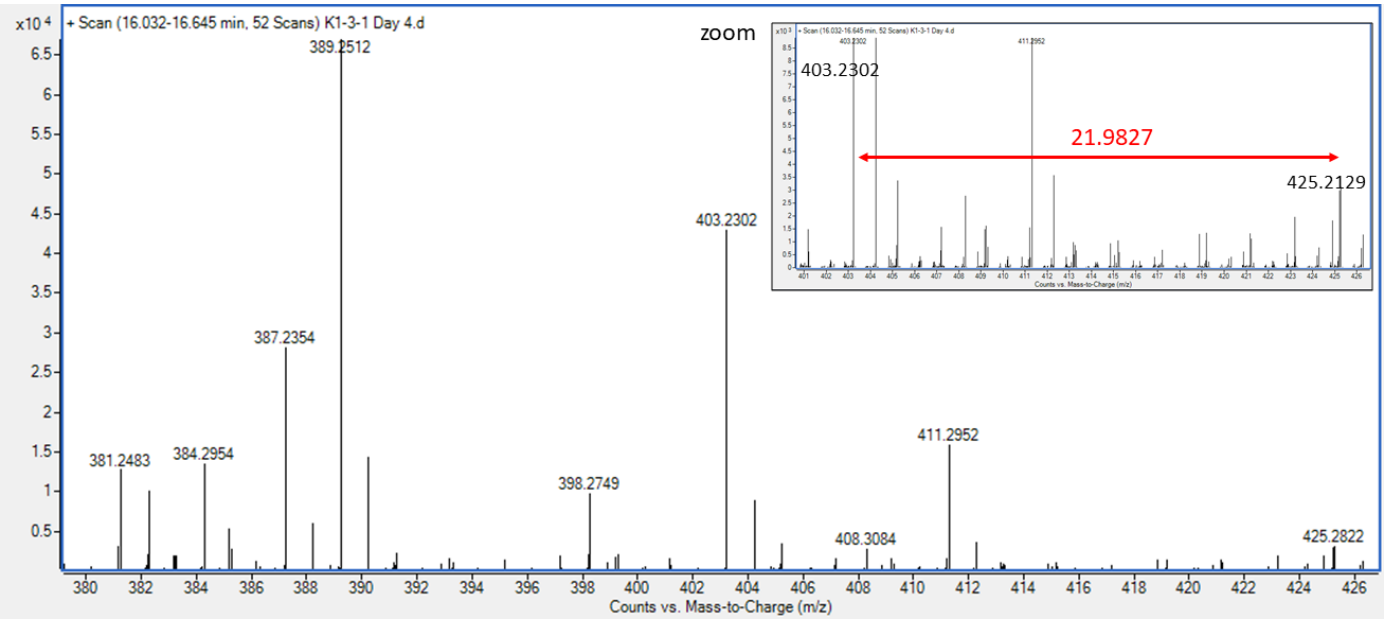

Figure S13. MS-MS of PPG-7-COOH for the proton adduct (*m/z* 439). The fragmentation pathway is shown in blue.

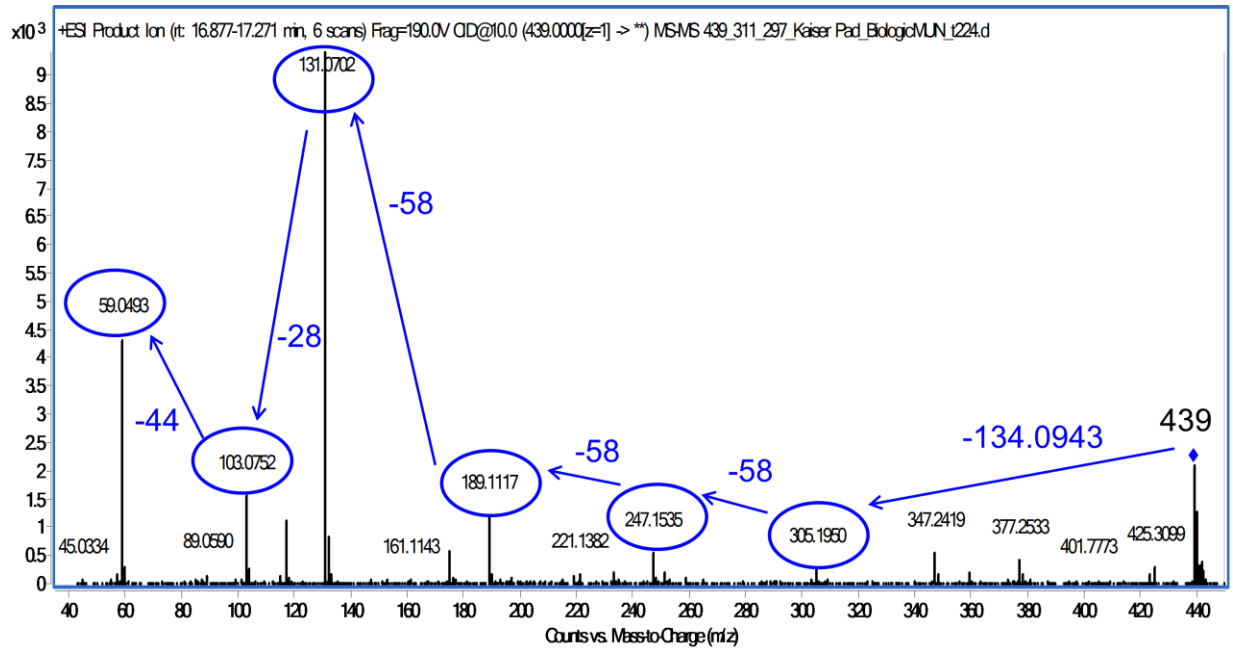

Figure S14. Relative abundance of *Pseudomonas* operational taxonomic unit (OTU) based on 16S rRNA gene analysis in the sediment microbial community from the A-22 (light blue circles), A-611 (dark blue triangles), and B-14 (green squares) microcosm experiments

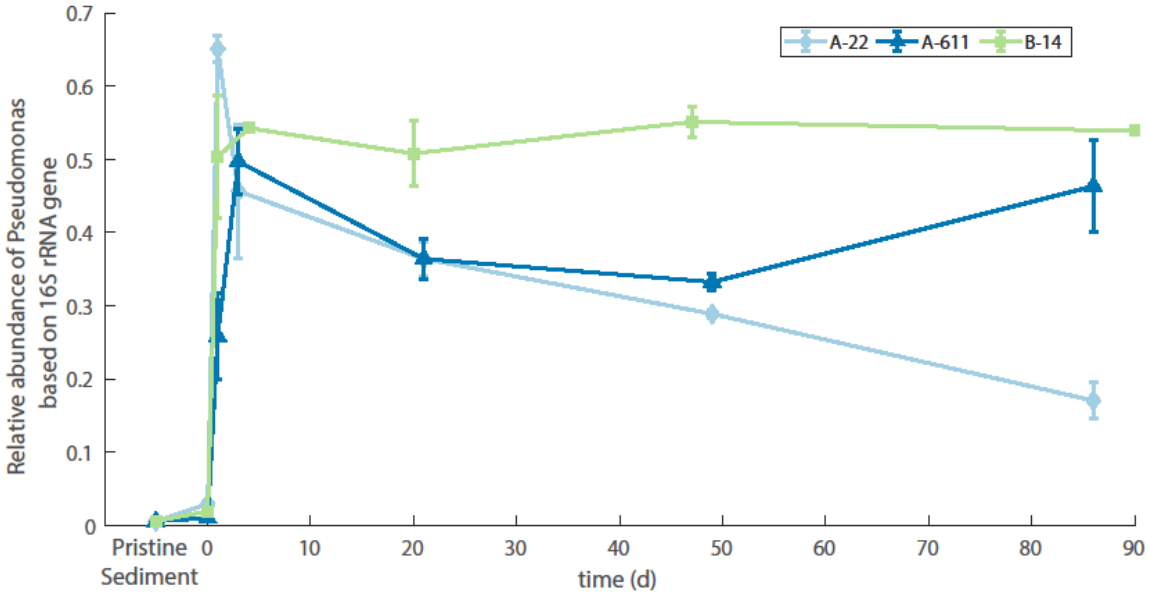

Figure S15. Relative response of PPG-4 (black circles) and corresponding product PPG-4-COOH (green squares) *vs.* time during the (a) A-22, (b) A-611, and (c) B-161 microcosm experiments. Response (integrated peak area) of the products is shown relative to the response of PPG-4 in the day 0 microcosm sample ($C/C_{0,parent}$).

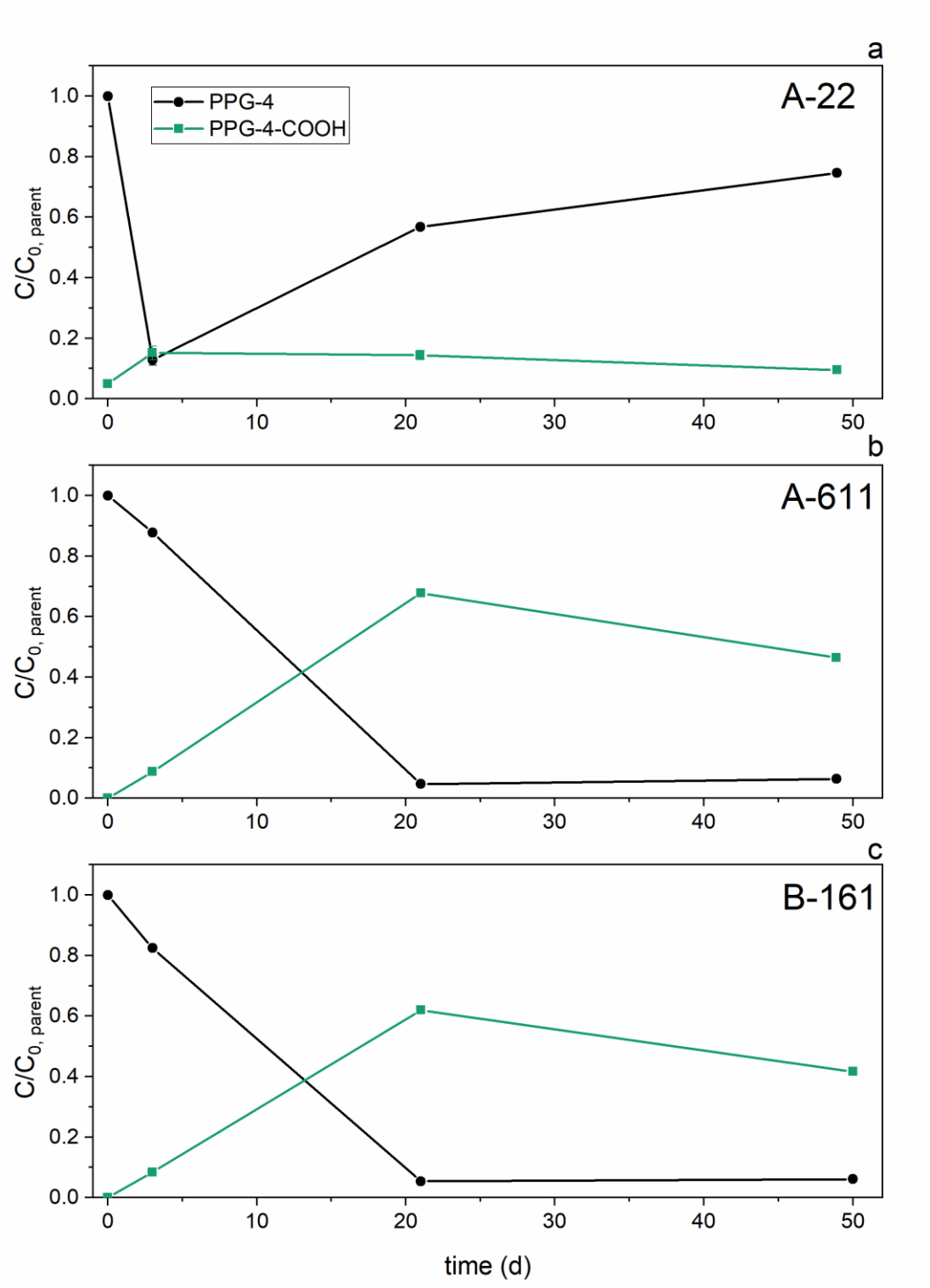

Figure S16. Relative response of PEG-9 (black circles) and corresponding products PEG-9-COOH (green squares) and PEG-9-diCOOH (orange diamonds) *vs.* time during the (a) A-22, (b) A-611, and (c) B-161 microcosm experiments. Response (integrated peak area) of the products are shown relative to the response of PEG-9 in the day 0 microcosm sample ($C/C_{0,parent}$).

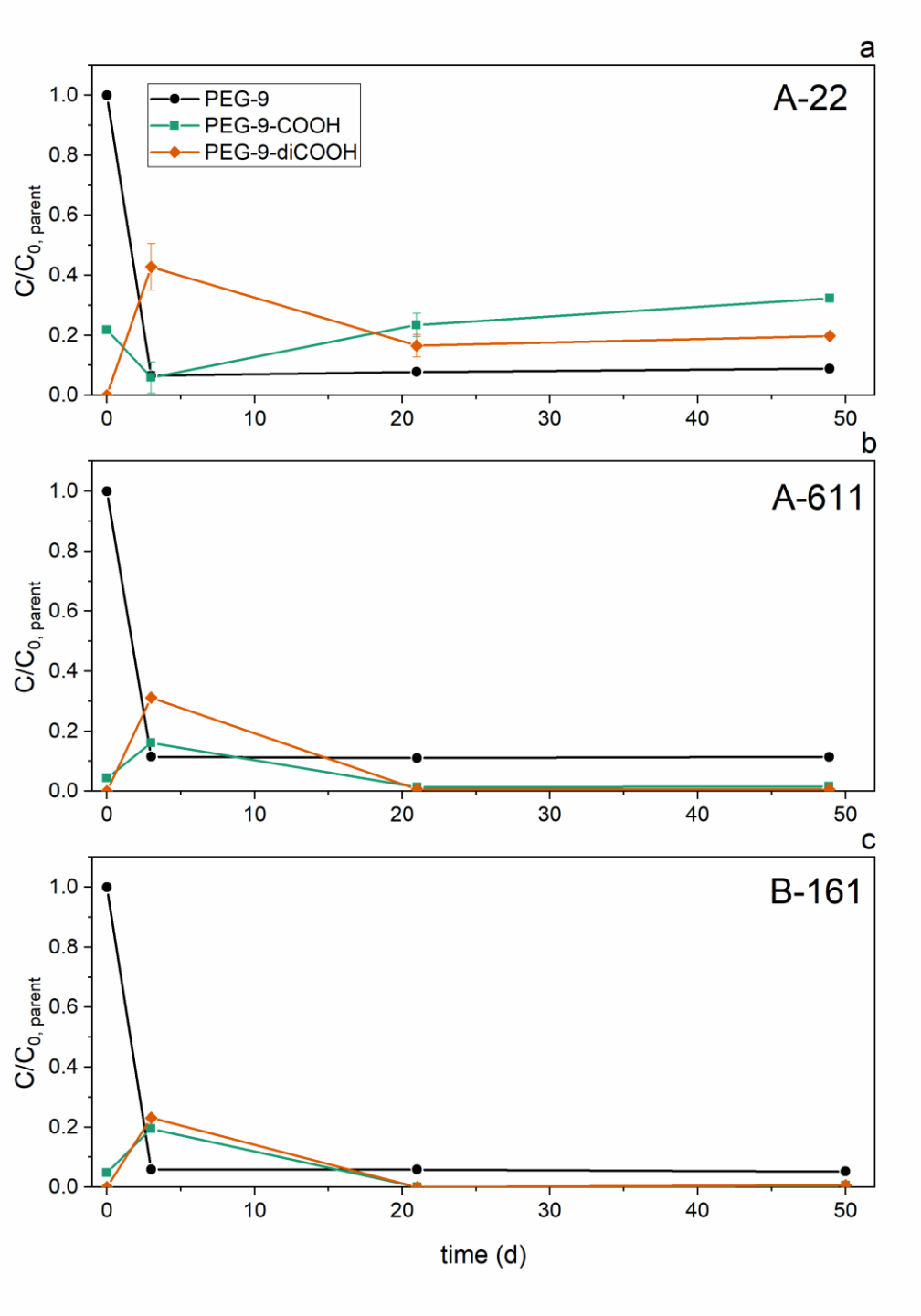

REFERENCES

(1) LuminUltra Technologies Ltd, *Test Kit Instructions: Quench-Gone Aqueous Test Kit,* New Brunswick, Canada, 2014.

(2) LuminUltra Technologies Ltd, *Test Kit Instructions: Deposit & Surface Analysis Test Kit,* New Brunswick, Canada, 2014.

(3) S. S. Paschke, ed, *Groundwater Availability of the Denver Basin Aquifer System, Colorado,* Professional Paper 1770, U.S. Geological Survey: Reston, Va., 2011.

(4) O. A., Sherwood, J. D. Rogers, G. Lackey, T. L. Burke, S. G. Osborn, J. N. Ryan, Groundwater methane in relation to oil and gas development and shallow coal seams in the Denver-Julesburg Basin of Colorado, *Proceedings of the National Academy of Sciences of the United States of America* 2016, **113**, 8391-8396.

(5) N. J. Bauch, M. Musgrove, B. J. Mahler, S. S. Paschke. *The quality of our Nation's waters-Water quality in the Denver Basin aquifer system, Colorado, 2003-05*, U.S. Geological Survey Circular 1357, U.S. Geological Survey: Reston, Virgina, 2014.

(6) J. P. Gustafsson, *Visual MINTEQ 3.0*. KTH Royal Institute of Technology: Stockholm, Sweden, 2012.

(7) K. J. Armstrong, J. D. Rogers, T. L. Burke and J. N. Ryan, Characterization of accidental spills and releases affecting groundwater in the Greater Wattenburg Area of the Denver-Julesburg Basin in northeastern Colorado, In *SPE Health, Safety, Security, Environment, & Social Responsibility Conference - North America*, Society of Petroleum Engineers, New Orleans, Louisiana, 18-20 April 2017, 2017.